In Vivo Adeno-Associated Viral Vector–Mediated Genetic Engineering of White and Brown Adipose Tissue in Adult Mice

Veronica Jimenez, Sergio Muñoz, Estefania Casana, Cristina Mallol, Ivet Elias, Claudia Jambrina, Albert Ribera, Tura Ferre, Sylvie Franckhauser, and Fatima Bosch

Adipose tissue is pivotal in the regulation of energy homeostasis through the balance of energy storage and expenditure and as an endocrine organ. An inadequate mass and/or alterations in the metabolic and endocrine functions of adipose tissue underlie the development of obesity, insulin resistance, and type 2 diabetes. To fully understand the metabolic and molecular mechanism(s) involved in adipose dysfunction, in vivo genetic modification of adipocytes holds great potential. Here, we demonstrate that adeno-associated viral (AAV) vectors, especially serotypes 8 and 9, mediated efficient transduction of white (WAT) and brown adipose tissue (BAT) in adult lean and obese diabetic mice. The use of short versions of the adipocyte protein 2 or uncoupling protein-1 promoters or micro-RNA target sequences enabled highly specific, long-term AAV-mediated transgene expression in white or brown adipocytes. As proof of concept, delivery of AAV vectors encoding for hexokinase or vascular endothelial growth factor to WAT or BAT resulted in increased glucose uptake or increased vessel density in targeted depots. This method of gene transfer also enabled the secretion of stable high levels of the alkaline phosphatase marker protein into the bloodstream by transduced WAT. Therefore, AAV-mediated genetic engineering of adipose tissue represents a useful tool for the study of adipose pathophysiology and, likely, for the future development of new therapeutic strategies for obesity and diabetes. ***Diabetes*** **62:4012–4022, 2013**

Obesity has become an alarming growing health problem, with more than 700 million people affected worldwide (1). Obesity increases the risk of mortality and is very strongly associated with insulin resistance and type 2 diabetes (2). Moreover, obesity is also an important risk factor for heart disease, immune dysfunction, hypertension, arthritis, neurodegenerative diseases, and certain types of cancer (3). Despite the clinical significance of obesity, no effective treatments are available, and additionally, antiobesity drugs often display important side effects due to their systemic actions (4). Hence, there is urgent need for novel and safe therapeutic approaches to block and reverse the current obesity epidemic. Unraveling of the pathological processes underlying obesity will be crucial for the development of new antiobesity therapies.

Deregulation of metabolic and endocrine functions of white adipose tissue (WAT), as well as impaired brown adipose tissue (BAT) activity and/or decreased mass, are considered among the main contributors to obesity and type 2 diabetes in experimental animal models and in humans (5–7). Genetic engineering of adipose cells offers great potential as a tool to study the molecular mechanisms underlying these pathogenic processes. However, immortalized white and brown murine adipocyte precursor cell lines, such as 3T3-L1, 3T3-F442A, BFC-1, and HB2, the most prominent cellular models used to study adipocyte differentiation and fat cell function in vitro, cannot easily be manipulated for efficient transfection (8), and adenovirus vector–mediated transduction of these cells is not efficient (9). Primary cultures of murine adipocytes are also refractory to transfection and electroporation (10), and cellular integrity is often compromised by the exposure to adenoviral vectors (11). Moreover, the transcriptional profile and the metabolic state of cultured immortalized precursor cell lines and primary adipocytes may differ substantially from those of adipocytes in vivo (12–15).

These facts highlight the need for a technology allowing for the genetic modification of adipose tissue in vivo. Numerous conventional and Cre-Lox and/or tetracycline-dependent genetically engineered mouse models in which transgene expression/deletion has been targeted specifically to WAT and/or BAT have been generated and constitute very useful experimental models (16). However, a main limitation of these models is that the gene of interest is normally overexpressed or downregulated throughout embryonic development and life span, which is not physiological (17–19). In addition, the technology required to obtain these animal models is complex, time-consuming, and costly because large cohorts of mice need to be generated.

Efficient in vivo gene transfer to WAT and BAT of adult mice could represent a solution to the issues of avoiding undesired effects on the embryo development and restricting transgene expression to a specific temporal window. This goal has not been achieved to date. Nonviral methods, such as electroporation, are very inefficient for in vivo gene transfer to white and brown adipocytes (20,21). Adenoviral vectors are able to transduce white adipocytes in vivo, but their high immunogenicity precludes long-term expression of the transgene (22). Long-term expression has been obtained with defective herpes simplex virus–derived vectors, although these vectors proved to be cytotoxic for preadipocytes and adipocytes (23).

From the Center of Animal Biotechnology and Gene Therapy and Department of Biochemistry and Molecular Biology, School of Veterinary Medicine, Universitat Autònoma de Barcelona, Bellaterra, and Centro de Investigación Biomédica en Red de Diabetes y Enfermedades Metabólicas Asociadas, Barcelona, Spain.

Corresponding author: Fatima Bosch, fatima.bosch@uab.es.

Received 22 February 2013 and accepted 6 September 2013.

DOI: 10.2337/db13-0311

This article contains Supplementary Data online at http://diabetes.diabetesjournals.org/lookup/suppl/doi:10.2337/db13-0311/-/DC1.

S.M. and E.C. contributed equally to this work.

Adeno-associated viral (AAV) vectors have emerged as one of the vectors of choice for many gene transfer applications in vivo because of their low immunogenicity and excellent safety profile (24). AAV vectors transduce dividing and nondividing cells, driving long-term gene expression (up to several years) in small- and large-animal models of disease in tissues with very low proliferation rates (24). Several AAV serotypes with a different cell tropism have been identified. AAV vectors of serotype 1 (AAV1) have been shown to modestly transduce mouse WAT in vivo when combined with nonionic surfactants and/or a proteosome inhibitor (25,26). The efficacy of other AAV serotypes in transducing WAT and BAT has not been explored yet.

In this study, we assessed the ability of AAV vectors of serotypes 1, 2, 4, 5, 6, 7, 8, and 9 to transduce murine WAT and BAT in vivo. Our results show that AAV8 and AAV9 vectors mediated long-term, efficient gene transfer to WAT and BAT after administration to adult mice, allowing for the induction of functional changes in adipocytes. This work demonstrates the value that AAV vectors hold as new tools for the genetic engineering of adipose tissue, which could be used in metabolic and pathophysiology studies as well as in the development of new therapies for obesity and type 2 diabetes.

RESEARCH DESIGN AND METHODS

Animals. Male ICR mice (8–12 weeks old), C57Bl/6J mice (9–13 weeks old), and B6.V-*Lep*^{ob}/OlaHsd (*ob/ob*) and BKS.Cg-+ *Lepr*^{db}/+ *Lepr*^{db}/OlaHsd (*db/db*) mice (8 weeks old) were used. Animal care and experimental procedures in this study were approved by the Universitat Autònoma de Barcelona Ethics Committee in Animal and Human Experimentation.

Recombinant AAV vectors. Single-stranded AAV vectors were produced by triple transfection of human embryonic kidney 293 cells and purified by a CsCl-based gradient method (27). Transgenes used were:

A. Enhanced green fluorescent protein (GFP) driven by *1*) the cytomegalovirus (CMV) early enhancer/chicken beta actin (CAG) promoter; *2*) the CAG promoter with the addition of four tandem repeats of the mirT122a sequence (5′CAAACACCATTGTCACACTCCA3′), the mirT1 sequence (5′TTACATACTTCTTTACATTCCA3′) or both, cloned in the 3′ untranslated region of the expression cassette; *3*) the short version of the adipocyte protein 2 (mini/aP2) promoter (28,29); or *4*) the short version of the uncoupling protein-1 (mini/UCP1) promoter (30,31);
B. Hexokinase 2 (HK2) driven by *1*) the CMV promoter, *2*) the mini/aP2 promoter, or *3*) the mini/UCP1 promoter;
C. Placental-derived secreted alkaline phosphatase (SeAP) driven by the mini/aP2 promoter;
D. Vascular endothelial growth factor (VEGF)-164 driven by the mini/UCP1 promoter; and
E. Red fluorescent protein (RFP), driven by the CMV promoter.

A noncoding plasmid carrying the CMV promoter, the mini/aP2 promoter, or the mini/UCP1 promoter and a multicloning site was used to produce null particles.

Administration of AAV vectors. Mice were anesthetized with ketamine (100 mg/kg) and xylazine (10 mg/kg). For the intraepididymal (intrae) WAT delivery, a laparotomy was performed. To distribute the vector in the whole depot, each epididymal fat pad was injected twice with 50 μL AAV solution. For intrainterscapular (intrai)BAT and intrainguinal (intrai)WAT administrations, a longitudinal incision in the skin at the interscapular or inguinal area was performed, respectively. To distribute the vector in the whole depot, each interscapular BAT (iBAT) or inguinal WAT (iWAT) received four injections of 10 μL AAV solution using a Hamilton syringe. For the systemic administration, AAV vectors were diluted in 200 μL saline and injected into the lateral tail vein.

Immunohistochemistry. Tissues were fixed for 12–24 h in 10% formalin, embedded in paraffin, and sectioned. Sections were incubated overnight at 4°C with a goat anti-GFP antibody (Abcam, Cambridge, MA), with a rabbit anti-RFP antibody (Abcam), with a goat anti-CD105 antibody (R&D Systems Inc., Minneapolis, MN) or with a mouse anti–α-smooth muscle actin (SMA) antibody (Sigma-Aldrich, Saint Louis, MO). A biotinylated donkey anti-goat antibody (Santa Cruz Biotechnology, Inc., Santa Cruz, CA), a biotinylated goat anti-rabbit antibody (Pierce Biotechnology, Inc., Rockford, IL), or a biotinylated horse anti-mouse antibody (Vector Laboratories, Burlingame, CA) was used as a secondary antibody. Streptavidin Alexa Fluor 488 (Molecular Probes; Life Technologies Corp., Carslbad, CA) was used as fluorochrome, and Hoechst (Sigma-Aldrich) was used for nuclear counterstaining. Alternatively, an ABC peroxidase kit (Pierce) was used, and sections were counterstained in Mayer's hematoxylin. Neutrophils were stained using a Naphthol AS-D Chloroacetate (Specific Esterase) kit (Sigma-Aldrich).

Measurement of GFP content. Tissues were disrupted in 1 mL lysis buffer (50 mmol/L Tris, 1% Nonidet P40, 0.25% sodium deoxycholate, 150 mmol/L NaCl, 1 mmol/L EDTA, in PBS, pH 7.4, sterile filtered) with a tissue homogenizer and incubated for 10 min at room temperature. After incubation, samples were centrifuged at 14,000 rpm for 10 min. GFP content was measured by luminescence in 100 μL supernatant using a 488-nm excitation wavelength and 512-nm emission wavelength (Flx800; BioTek Instruments, Inc., Winooski, VT). GFP content values were corrected by total protein content of the sample.

Isolation of adipocytes. AAV-transduced adipocytes were isolated using a modification of the Rodbell method (32). Isoflurane-anesthetized mice were killed by decapitation, and epididymal WAT (eWAT) was minced and digested at 37°C in Krebs-Ringer bicarbonate HEPES buffer (KRBH) containing 4% BSA (fatty acid-free), 0.5 mmol/L glucose, and 0.5 mg/mL collagenase type II (C6885; Sigma-Aldrich) during 35–45 min. Fat cells were isolated by gentle centrifugation and washed three times with fresh collagenase-free KRBH without glucose.

RNA analysis. Total RNA was obtained from isolated adipocytes or adipose tissue samples using QIAzol Lysis Reagent (Qiagen, Hilden, Germany) and RNeasy Lipid Tissue Minikit (Qiagen). To eliminate residual viral genomes (vg), total RNA was treated with DNAseI (Qiagen). For RT-PCR, 1 μg RNA was reverse-transcribed using the Transcriptor First Strand cDNA Synthesis kit (Roche Diagnostic GmbH, Roche Applied Science, Mannheim, Germany). Quantitative PCR was performed in a LightCycler 480 II (Roche) using the LightCycler 480 SYBR Green I Master kit (Roche). The sequences of the sense and antisense oligonucleotides primers used were: GFP, 5′AAGTTCATCTGCACCACCG3′, 5′TCCTTGAAGAAGATGGTGCGC3′; RFP, 5′GCGGCCACTACACCTGCGAC3′, 5′TCGGCGTGCTCGTACTGCTC3′; HK2, 5′GAAGGGGCTAGGAGCTACCA3′, 5′CTCGGAGCACACGGAAGTT3′; SeAP, 5′CGGCTGTTGGGCACTGA3′, 5′GGAAGGTCCGCTGGATTGA3′; VEGF164, 5′AGACAGAACAAAGCCAGAAACTCAC3′, 5′CACGTCTGCGGATCTTGGAC3′; platelet endothelial cell adhesion molecule 1 (PECAM1), 5′CTGGTGCTCTATGCAAGCCTC3′, 5′CGGTGCTGAGACCTGCTTT3′; adiponectin, 5′TGTTCCTCTTAATCCTGCCCA3′, 5′CCAACCTGCACAAGTTCCCTT3′; leptin, 5′GAGACCCCTGTGTCGGTTC3′, 5′CTGCGTGTGTGAAATGTCATTG3′; resistin, 5′AACTCCCTGTTTCCAAATGC3′, 5′AGCAGCTCAAGACTGCTGTG3′; interleukin (IL)-6, 5′CATGGATGCTACCAAACTGGAT3′, 5′CCAGGTAGCTATGGTACTCCAGA3′, IL-1β, 5′TGTAATGAAAGACGGCACACC3′, 5′TCTTCTTTGGGTATTGCTTGG3′; and monocyte chemoattractant protein-1 (MCP-1), 5′CCCAATGAGTAGGCTGGAGA3′, 5′TCTGGACCCATTCCTTCTTG3′. Data were normalized with 36B4 values (33).

Glucose uptake ex vivo in isolated adipocytes. Glucose uptake in isolated adipocytes was measured at different insulin concentrations. Isolated adipocytes were obtained by collagenase digestion of eWAT from fed mice, as described above. The adipocyte suspension (250 μL) was incubated with KRBH plus 4% BSA (fatty acid-free), 10 mmol/L of the deoxy-D-glucose, 0.4 μCi of 2-[1-^{3}H]deoxy-D-glucose (2DG) (PerkinElmer, Waltham, MA), and different insulin concentrations for 5 min. Afterward, adipocytes and incubation medium were separated through silicon oil (Sigma-Aldrich) in polypropylene tubes, and radioactivity in the adipocyte samples was assessed by liquid scintillation counting. The results were expressed as picomoles of 2DG per 10^{6} cells per min.

Glucose uptake in vivo. The in vivo basal glucose utilization index was determined as previously described (34). Briefly, 4 μCi 2DG (PerkinElmer) was mixed in BSA-citrate buffer. A flash injection of radiolabeled mix was administered into the jugular vein of anesthetized (ketamine and xylazine) fed mice at time zero. The specific blood 2DG clearance was determined by the Somogyi procedure in 25 μL blood samples (tail vein) obtained 1, 15, and 30 min after injection. Tissue samples were removed 30 min after injection. The glucose utilization index was determined by measuring the accumulation of radiolabeled compounds. The amount of 2DG-6-phosphate per milligram of protein was divided by the integral of the concentration ratio of 2DG to unlabeled glucose measured. Because values were not corrected by a "discrimination constant" for 2DG in glucose metabolic pathways, the results are expressed as the index of glucose utilization, in picomoles per milligram of protein per minute.

Measurement of SeAP and adiponectin serum levels. Circulating human SeAP was quantified in 5 μL serum using the Tropix Phospha-Light System (Applied Biosystems, Inc.). Serum adiponectin was measured with a mouse/rat RIA Kit (Millipore, Billerica, MA).

Flow cytometry. eWAT and iBAT stroma vascular fraction, hepatic nonparenchymal cells, and peripheral blood mononuclear cells were isolated as previously described (35,36). F4/80 (BioLegend, San Diego, CA), CD3em, and NK-1.1 (BD Pharmigen, Franklin Lakes, NJ) antibodies were used. Flow cytometric analyses were performed on a FACSCanto flow cytometer (BD Biosciences, Franklin Lakes, NJ).

Statistical analysis. All values are expressed as mean ± SEM. Differences between groups were compared by the Student *t* test. Differences were considered significant at $P < 0.05$.

RESULTS

In vivo transduction of WAT by local delivery of AAV vectors. To asses the in vivo transduction efficiency of WAT by AAV vectors, AAV of serotypes 1, 2, 4, 5, 6, 7, 8 or 9 encoding the GFP under the control of the ubiquitous promoter CAG were injected into the eWAT in adult mice. Transduction efficiency of WAT was evaluated 2 weeks postinjection, given that at this time point AAV vectors have been reported to mediate robust transgene expression in most tissues. AAV8 and AAV9 vectors transduced the vast majority of adipocytes in eWAT, outperforming AAV1, 2, 4, 5, 6, and 7 vectors (Fig. 1*A* and *B* and Supplementary Fig. 1*A)*. Similarly, local administration of AAV8 and AAV9-CAG-GFP vectors into the iWAT mediated extensive transduction of white and beige adipocytes in this depot (Fig. 1*C* and *D*).

The intraeWAT and intraiWAT administration of AAV8 or AAV9 vectors also resulted in transduction of the liver and heart (Supplementary Fig. 1*B* and data not shown). To restrict transgene expression to adipose tissue, we used murine mini/aP2, which allowed overcoming the limited cloning capacity of AAV vectors (4.7 kb). This promoter comprises the basal promoter and adipocyte-specific enhancer of aP2 (28,29). The intraeWAT administration of AAV8 or AAV9-mini/aP2-GFP vectors mediated specific transduction of white adipocytes (Supplementary Fig. 1*C*), with no detectable GFP expression in the liver and heart (Supplementary Fig. 1*D*) and iBAT (data not shown).

To demonstrate that in vivo AAV-mediated transduction of adipocytes may be a suitable model to study adipose function, AAV9 vectors encoding the murine HK2, the main glucose phosphorylating enzyme in fat cells, under the control of the ubiquitous CMV promoter (AAV9-CMV-HK2) or an equal dose of the AAV9-CMV-null vector, were delivered intraeWAT. Adipocytes isolated from AAV9-CMV-HK2–treated mice showed overexpression of HK2 compared with adipocytes obtained from AAV9-CMV-null–injected mice (Fig. 1*E*). Accordingly, in vitro insulin-stimulated 2DG uptake was increased in AAV9-CMV-HK2–transduced adipocytes compared with adipocytes from AAV9-CMV-null–treated animals (Fig. 1*F*). Furthermore, animals injected intraeWAT with AAV9-mini/aP2-HK2 vectors showed a greater increase (about threefold) in 2DG uptake in vivo than AAV9-mini/aP2-null–treated animals (Fig. 1*G*). As expected, no differences in 2DG uptake were detected between groups in iBAT and heart (Fig. 1*G*).

Finally, to test the ability of AAV-engineered eWAT to secrete proteins of interest into the bloodstream, human SeAP was used as reporter. AAV9-mini/aP2-SeAP vectors were injected bilaterally intraeWAT, and a long-term follow-up of circulating SeAP was performed. At 2 weeks after AAV vector delivery, high levels of SeAP were detected in serum. Levels rose progressively up to day 30 and thereafter remained stable for the duration of the study (>140 days) (Fig. 1*H*).

In vivo genetic engineering of BAT by local delivery of AAV vectors. Upon intraiBAT administration of AAV8 or AAV9-CAG-GFP vectors, numerous GFP^+ brown adipocytes were detected throughout the depot (Fig. 2*A*). Quantification of transduction efficiency showed that AAV8 and AAV9 were as efficient as AAV7 and superior to AAV1, AAV2, and AAV5 vectors in transducing iBAT (Fig. 2*B*).

The intraiBAT administration of AAV7, AAV8, or AAV9 vectors also resulted in gene transfer to the liver and heart (Supplementary Fig. 2*A*). To restrict transgene expression to iBAT, the mini/UCP1 promoter was used. The mini/UCP1 promoter comprises the basal promoter and the adipose-specific enhancer of rat UCP1 (30,31). The intraiBAT administration of AAV8 or AAV9-mini/UCP1-GFP achieved efficient transduction of brown adipocytes (Fig. 2*C*), abolished transgene expression in the heart, and mediated very marginal liver transduction (Supplementary Fig. 2*B*), in agreement with previous reports (31).

Animals treated locally with AAV8-mini/UCP1-HK2 showed increased in vivo 2DG uptake in iBAT compared with AAV8-mini/UCP1-null–treated animals (Fig. 2*D*). As expected, no difference was found between groups in the 2DG uptake in eWAT and heart (Fig. 2*D*). Similarly, animals injected intraiBAT with AAV9 vectors encoding the isoform 164 of murine VEGF (AAV9-mini/UCP1-VEGF164) showed marked overexpression of VEGF164 (Fig. 2*E*) and increased vessel density in this fat depot, as revealed by increased expression of PECAM1, a commonly used endothelial cell marker (36,37) (Fig. 2*E*), and increased immunostaining with CD105, a marker of proliferating endothelial cells (38) or with the pericyte marker α-SMA (39) (Fig. 2*F* and Supplementary Fig. 2*C*).

In vivo genetic engineering of WAT and BAT by systemic administration of vectors. The systemic delivery of AAV8 or AAV9 vectors transduces a wide variety of tissues (40,41). However, transduction of WAT and BAT by intravascular administration of these serotypes has never been reported before. After intravascular administration of 5×10^{12} vg of AAV8 or AAV9-CAG-GFP vectors to lean mice, white and brown fat depots of the whole body were transduced although transduction efficiencies in the different depots varied with mouse strain (Fig. 3*A*–*D*). Lower systemic doses of vectors (5×10^{10} and 5×10^{11} vg) also mediated gene transfer to WAT and BAT, although at reduced efficiency (Supplementary Fig. 3*A* and *B*). No sex differences were observed in AAV9-mediated transduction of the different adipose depots, except for gonadal fat pads (Supplementary Fig. 3*C*). Importantly, the intravascular administration of AAV8 or AAV9 vectors to diabetic obese *ob*/*ob* mice (Fig. 4*A* and *B*) or *db*/*db* mice (Fig. 4*C* and *D*) also resulted in the genetic engineering of WAT and BAT, with efficiencies similar to those attained in lean mice (Fig. 3*C* and *D*).

Noticeably, the intravascular administration of AAV8 or AAV9 vectors did not result in infiltration of WAT, BAT, or the liver with macrophages, T lymphocytes, or natural killer cells (Fig. 5*A*, *B* and Supplementary Fig. 4*A*), nor was neutrophilic infiltration detected in the liver (Supplementary Fig. 4*B*). Accordingly, no changes in the expression profile of adipokines and proinflammatory cytokines were detected in WAT (Fig. 5*C*), and circulating levels of adiponectin remained normal in AAV8- and AAV9-treated animals (Fig. 5*D*). Moreover, intravascular delivery of AAV8 or AAV9 vectors did not lead to transduction of

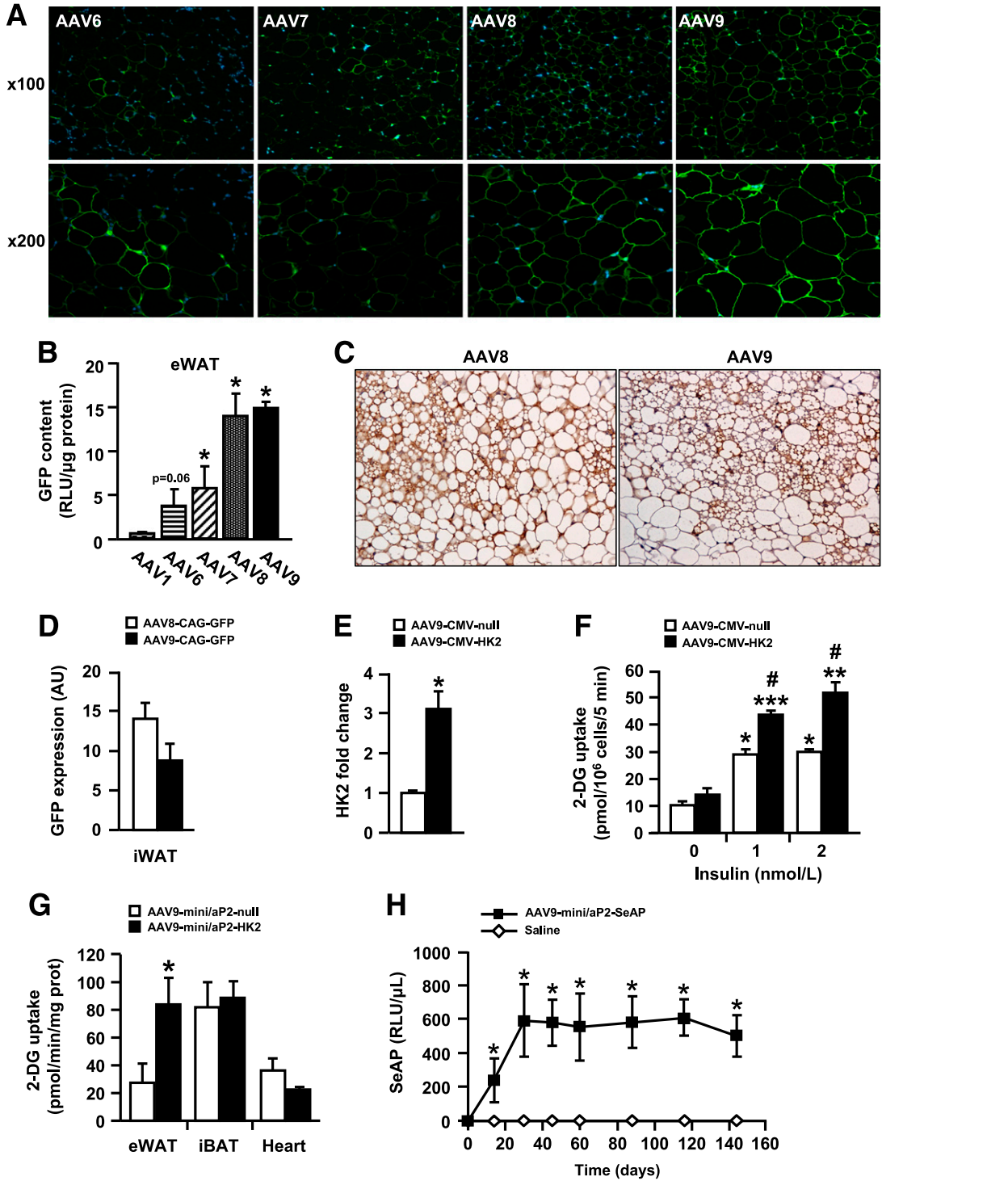

FIG. 1. Transduction of WAT after local administration of AAV vectors. *A*: Immunostaining against GFP (green) in sections of eWAT 2 weeks after the intraeWAT administration of 2×10^{11} vg of AAV-CAG-GFP vectors of serotypes 6, 7, 8, or 9. Blue, nuclei. Original magnification ×100 (*upper panel*) and ×200 (*lower panel*). *B*: GFP content in eWAT treated with 2×10^{11} vg of AAV-CAG-GFP vectors of serotypes 1, 6, 7, 8, or 9 at 2 weeks postinjection ($n = 5$ mice/group). *C*: Immunostaining against GFP (brown) in sections of iWAT 2 weeks after the intraiWAT administration of 2×10^{11} vg of AAV8 or AAV9-CAG-GFP vectors. Original magnification ×100. *D*: GFP expression levels in iWAT 2 weeks postinjection of 2×10^{11} vg of AAV8 or AAV9-CAG-GFP ($n = 6$). AU, arbitrary units. *E*: HK2 expression levels in adipocytes isolated 2 weeks after intraeWAT administration of 2×10^{11} vg of AAV9-CMV-HK2 or AAV9-CMV-null vectors ($n = 5$). *F*: In vitro basal and insulin-stimulated 2DG uptake by adipocytes isolated 2 weeks after intraeWAT administration of 2×10^{11} vg of AAV9-CMV-HK2 or AAV9-CMV-null vectors ($n = 5$). *G*: In vivo 2DG uptake by eWAT, iBAT, and heart 2 weeks after the intraeWAT injection of 1.4×10^{12} vg of AAV9-mini/aP2-null or AAV9-mini/aP2-HK2 vectors ($n = 7$). *H*: Follow-up of circulating levels of human SeAP in animals administered intraeWAT with 2×10^{12} vg of AAV9-mini/aP2-SeAP or saline ($n = 3$). Values shown are means ± SEM. RLU, relative light units. *$P < 0.05$, **$P < 0.01$, and ***$P < 0.001$; # $P < 0.05$ vs. AAV9-CMV-null at the same insulin concentration.

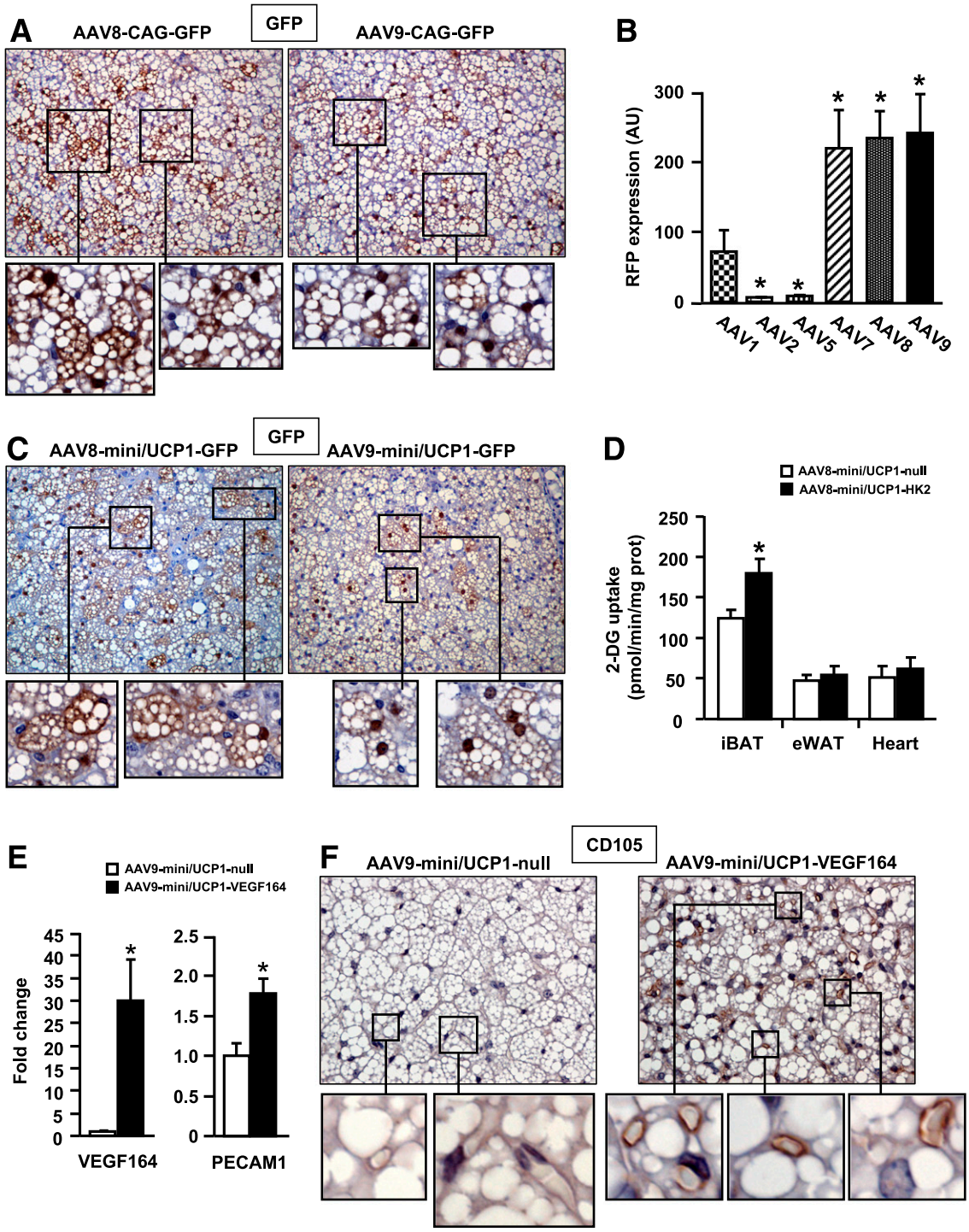

FIG. 2. Transduction of BAT after intraiBAT administration of AAV vectors. *A*: Immunostaining against GFP (brown) in sections of iBAT after intraiBAT administration of 2 × 10^9 vg of AAV8 or AAV9-CAG-GFP. Original magnification ×200 and ×400 (*insets*). *B*: RFP expression levels in iBAT after administration of 10^{10} vg of AAV-CMV-RFP vectors of serotypes 1, 2, 5, 7, 8, or 9 (n = 3–5 mice/group). AU, arbitrary units. *C*: Immunostaining against GFP (brown) in sections of iBAT administered with 2 × 10^{11} vg of AAV8 or AAV9-mini/UCP1-GFP. Original magnification ×200 and ×400 (*insets*). *D*: In vivo 2DG uptake by iBAT, eWAT, and heart after intraiBAT administration of 7 × 10^{10} vg of AAV8-mini/UCP1-HK2 (n = 6) or AAV8-mini/UCP1-null vectors (n = 10). *E*: VEGF164 and PECAM1 expression levels in iBAT after intraiBAT administration of 2 × 10^{11} vg of AAV9-mini/UCP1-VEGF164 or AAV9-mini/UCP1-null vectors (n = 5). *F*: Immunostaining against CD105 (brown) in iBAT from the same cohorts. Original magnification ×400 and ×1,000 (*insets*). All analyses were performed 2 weeks after vector administration. Values shown are means ± SEM. *$P < 0.05$.

macrophages in eWAT, iBAT, the liver or peripheral blood (data not shown).

We then tested whether the mini/aP2 and mini/UCP1 promoters could be used to restrict transgene expression to white and/or brown adipocytes after systemic delivery of AAV vectors. The intravascular administration of AAV9-mini/aP2-GFP or AAV9-mini/UCP1-GFP vectors attained highly adipose-specific GFP expression in white and/or

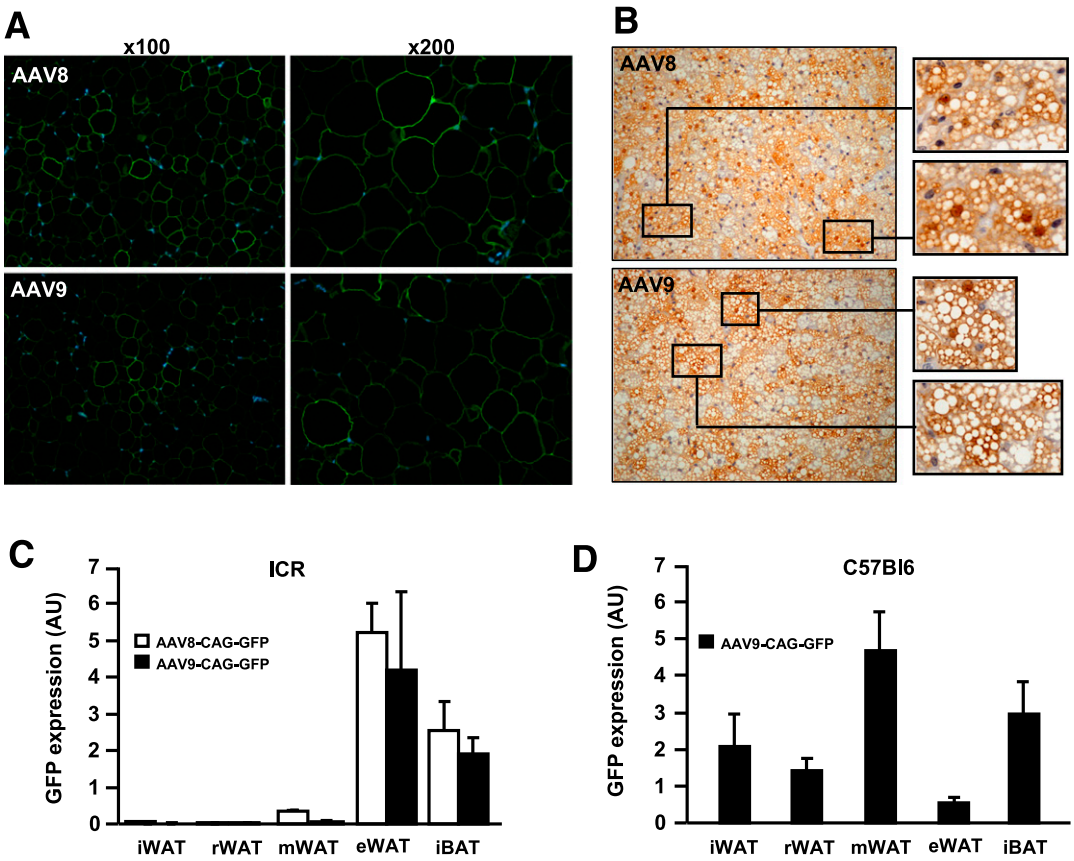

FIG. 3. Transduction of WAT and BAT after systemic administration of AAV vectors to lean mice. Tail vein injection was used to deliver 5 × 10^{12} vg of AAV8- or AAV9-CAG-GFP vectors to lean mice, and samples were analyzed 2 weeks after vector administration. *A*: Immunostaining against GFP (green) in eWAT. Blue, nuclei. Original magnification ×100 (*left panels*) and ×200 (*right panels*). *B*: Immunostaining against GFP (in brown) in iBAT sections. Original magnification ×200 and ×400 (*insets*). Relative GFP expression levels in iWAT, retroperitoneal WAT (rWAT), mesenteric WAT (mWAT), eWAT, and iBAT fat depots after intravascular administration of vectors to ICR mice (*C*) and C57Bl6 mice (*D*) (ICR: *n* = 3 for AAV8 and *n* = 5 for AAV9; C57Bl6: *n* = 4). Values shown are means ± SEM. AU, arbitrary units.

brown adipocytes, respectively (Fig. 6*A* and *B*), with no detectable transgene expression in the heart and very marginal transduction of the liver, which presented only a few scattered GFP^+ hepatocytes (Supplementary Fig. 5*A*). Similar results were obtained for the AAV8 serotype (data not shown). However, the level of transgene expression mediated by the mini/aP2 or mini/UCP1 promoters was much lower than that afforded by the CAG promoter (Supplementary Fig. 5*B*). Nevertheless, systemic administration of AAV9-mini/UCP1-VEGF164 resulted in increased expression of VEGF164 and PECAM1 (Fig. 6*B* and *C*) and increased vessel density (Fig. 6*D* and *E*) in iBAT.

To further strengthen the potential of AAV vectors to genetically modify adipose tissue when administered systemically and given the reduced transgene expression attained by the mini/aP2 and mini/UCP1 promoters, we also investigated the use of the CAG promoter in conjunction with tissue-specific micro-RNA target (miRT) sequences in an attempt to obtain high expression levels in adipose tissue and de-target transgene expression from off-target organs. Upon intravascular administration of AAV9-CAG-GFP vectors containing targets of the liver-specific miR122a (AAV9-CAG-GFP-miRT122) (42), the heart-specific miR1 (AAV9-CAG-GFP-miRT1) (43) or both (AAV9-CAG-GFP-doublemiRT), high levels of GFP expression were observed in white and brown adipocytes, whereas GFP production in the liver and/or heart, respectively, was nearly completely abolished (Fig. 7).

DISCUSSION

In this study, we have shown that local or systemic administration of AAV vectors, especially serotypes 8 and 9, leads to robust genetic engineering of white and brown adipocytes in adult mice. The systemic administration of AAV8 or AAV9 vectors mediated transduction of whole-body adipose depots in lean and obese diabetic mice. However, depending on the strain, variable transduction efficiencies among depots were observed. Distinct WAT depots are not equivalent, because developmental, morphological, molecular, and functional differences among them have been reported for mice and humans (44,45). The differences observed in transduction efficiencies between depots may be also due to their distinct degree of vascularization. Indeed, retroperitoneal and inguinal depots are less vascularized than the rest of the fat pads, being that inguinal depots have the lowest density of blood vessels (46). Although high vascular density and blood flow have been described in the mesenteric depot (46), this fat pad also contains a large amount of structural and extracellular proteins that modulate cell–cell and cell–matrix adhesion and endothelial permeability (47), which may impair genetic engineering of this depot by systemic administration of AAV vectors. Moreover, the delivery route may also substantially influence transduction efficiency. In this regard, when AAV vectors were administered intradepot to eWAT, iWAT, and iBAT, efficient transduction of adipocytes was observed.

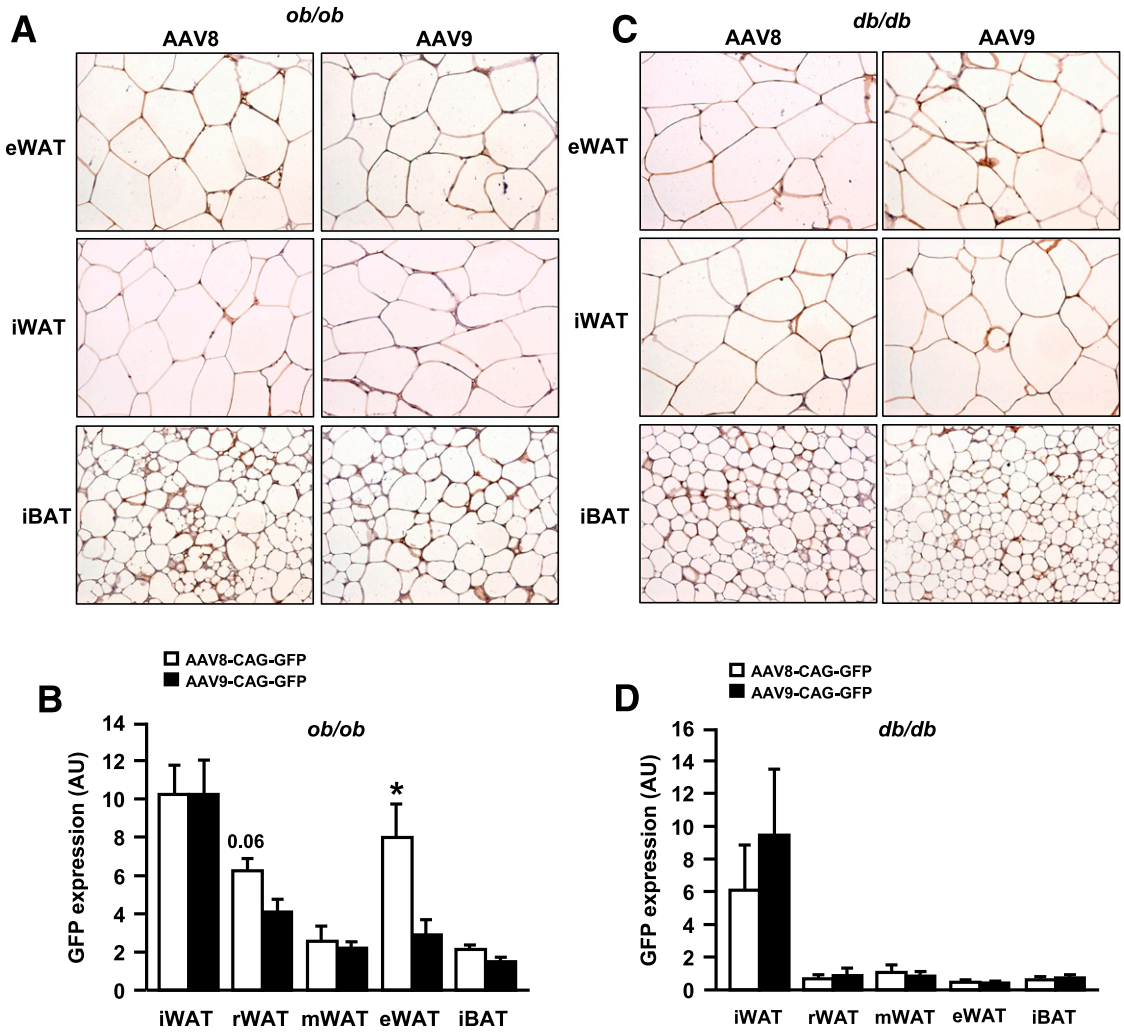

FIG. 4. Transduction of WAT and BAT after systemic administration of AAV vectors to obese diabetic mice. Immunostaining against GFP (brown) in eWAT, iWAT, and iBAT sections after intravascular administration of 3×10^{12} vg of AAV8- or AAV9-CAG-GFP vectors to *ob/ob* ($n = 4$) (*A*) and *db/db* ($n = 4$) mice (*C*). Original magnification ×200. GFP expression in inguinal (iWAT), retroperitoneal (rWAT), mesenteric (mWAT), eWAT, and iBAT depots from the same cohorts of *ob/ob* (*B*) and *db/db* mice (*D*). All analyses were performed 2 weeks after vector delivery. Values shown are means ± SEM. *$P < 0.05$ vs. AAV9. AU, arbitrary units.

Local administration of AAV7, AAV8, and AAV9 vectors also resulted in transduction of nonadipose tissues because these serotypes can cross endothelial barriers and reach the bloodstream (41). The use of the mini/aP2 and mini/UCP1 promoters or the liver and heart-specific mirT sequences prevented to a great extent transgene expression in off-target organs and afforded long-term transgene expression after local or systemic delivery of AAV vectors. Moreover, overexpression of HK2 or VEGF164 mediated by AAV-mini/aP2 or AAV-mini/UCP1 resulted in WAT- or BAT-specific increased in vivo glucose uptake or vascular density, respectively. Similar results have been observed using transgenic mice overexpressing VEGF164 in BAT (36,37) or the glucose phosphorylating enzyme glucokinase in WAT (32), highlighting the potential of AAV vectors to achieve genetic engineering of adipose tissue in adult mice. Thus, this gene transfer methodology may be an attractive alternative to the use of adipose-specific transgenic/knock-out mouse models, especially when high-throughput screening of genes is required. Furthermore, the aP2 promoter, which is frequently used to achieve adipocyte-specific expression of genes of interest in transgenic models, conveys transcription in cell types other than adipocytes, such as macrophages and cardiomyocytes (48). Conversely, the mini/aP2 promoter precluded transduction of the heart, and AAV8 and AAV9 vectors did not mediate genetic engineering of macrophages, consistent with the poor tropism of these serotypes for this cell type (35,49). Additional advantages of the strategy presented here over the use of transgenic animals are that AAV vector production can be done in a relatively short period of time (a few weeks), discrete depots of choice can be engineered by intradepot administration, and the same vector construct can be tested in different animal models of obesity and diabetes, including large-animal models (50).

Numerous experimental and clinical studies have documented that AAVs, in contrast to other types of vectors, such as adenoviruses, have very mild proinflammatory potential due to their inability to efficiently trigger innate immune responses (51,52). One recent study, however, reported infiltration and production of proinflammatory

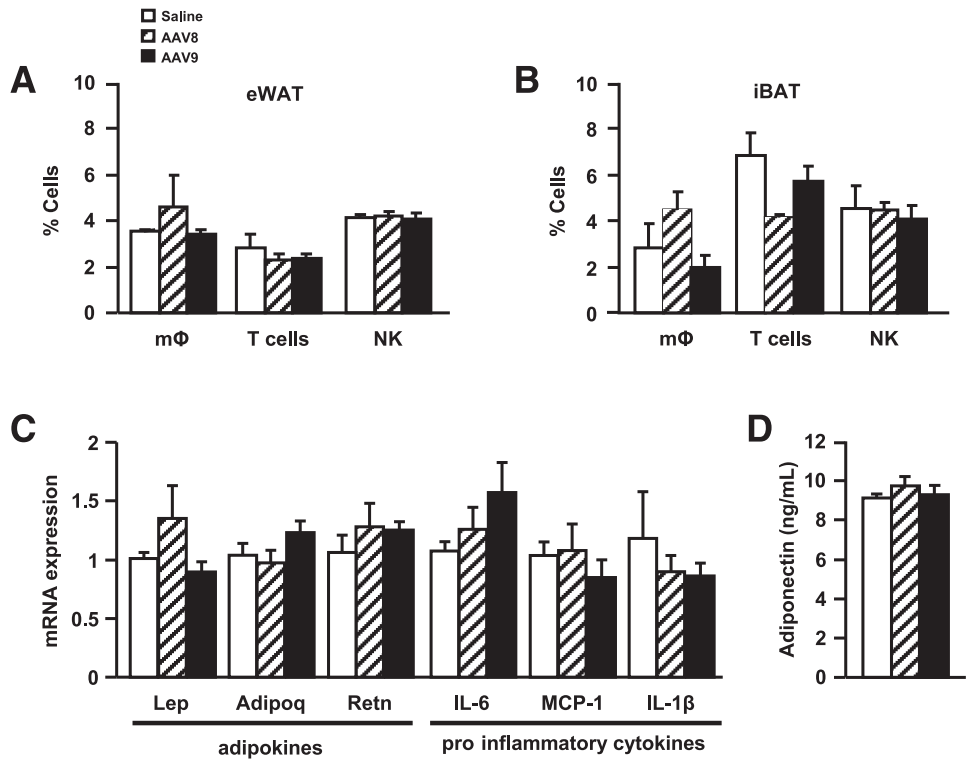

FIG. 5. Assessment of adipose tissue inflammation after systemic administration of AAV vectors. Flow cytometric quantification of the number of macrophages (mΦ), T lymphocytes (T cells), and natural killer cells (NK) in eWAT (*A*) and iBAT (*B*) 1 month after intravascular administration of 3×10^{12} vg of AAV8 or AAV9-CAG-GFP to C57Bl6 mice (n = 3–4). *C*: Relative expression of adipokines and proinflammatory cytokines in eWAT at 2 weeks after intravascular administration of 2×10^{12} vg of AAV8 or AAV9-CAG-null vectors to C57Bl6 mice (n = 7–8). Lep, leptina; Adipoq, adiponectin; Retn, resistin. *D*: Serum adiponectin levels in the same cohorts. Values shown are means ± SEM.

cytokines in the liver after intravascular administration of AAV vectors in mice, although these responses were boosted by double-stranded and not by single-stranded AAV vectors (53). Our results clearly show that intravascular administration of single-stranded AAV8 or AAV9 vectors does not lead to inflammation of the liver or adipose tissue.

Much of the research on fat cell function and differentiation published to date has relied on the use of primary adipocyte cultures and immortalized adipocyte precursor cell lines in vitro. However, not all precursor cells undergo differentiation, and mature adipocytes derived from these cell lines present remarkable phenotypic differences compared with wild-type adipocytes, such as aneuploidy, altered pattern of fat deposition, aberrant gene expression, and decreased insulin sensitivity (12–15). Gene transfer to the vast majority of these in vitro models is also inefficient, and primary adipocytes cannot be maintained in culture for long periods of time. In our study, AAV8 and AAV9 vectors mediated efficient, long-term transduction of white and brown adipocytes in vivo. Furthermore, the intra-eWAT administration of AAV9-CMV-HK2 vectors led to increased glucose uptake when measured in vitro in isolated adipocytes. Thus, in vivo genetic engineering of adipose tissue by AAV vectors, followed by isolation of the engineered adipocytes, may be a useful approach to perform gene function studies in fat cells in vitro, because it would allow the use of efficiently transduced, bona fide adipocytes. Moreover, the isolation of in vivo transduced adipocytes weeks or months after vector delivery would also allow in vitro studies that require long-term genetic modification.

AAV-mediated genetic engineering of adipose tissue may also open up new opportunities for the development of future therapeutic strategies to treat obesity and type 2 diabetes. To this end, the safety and efficacy of AAV-mediated gene transfer has been extensively studied in humans, with encouraging results in the liver, muscle, central nervous system, and retina (24). Thus, AAV-mediated gene therapy approaches targeting obesity-specific alterations, such as WAT inflammation and hypoxia or thermogenesis, may constitute attractive therapeutic strategies.

The high secretory capacity shown by AAV-modified WAT may be exploited for the development of new gene therapy strategies for diseases in which supply of the therapeutic agent into the bloodstream is needed for treatment/cure, such as hemophilia (24), diabetes (50) or lysosomal storage diseases (40). Our data suggest that AAV-modified WAT can act as a "therapeutic pump" and, therefore, become an attractive target site in alternative to the liver and muscle, given its accessibility and the possibility of easy surgical removal of WAT if unexpected events occurred. This possibility may be of significant importance for patients who are not eligible for liver-directed gene transfer because of underlying hepatic disease, such as hemophilia patients with liver failure, cirrhosis, or liver cancer due to hepatitis C.

In summary, our findings demonstrate that AAV vectors offer great potential for the long-term postnatal genetic

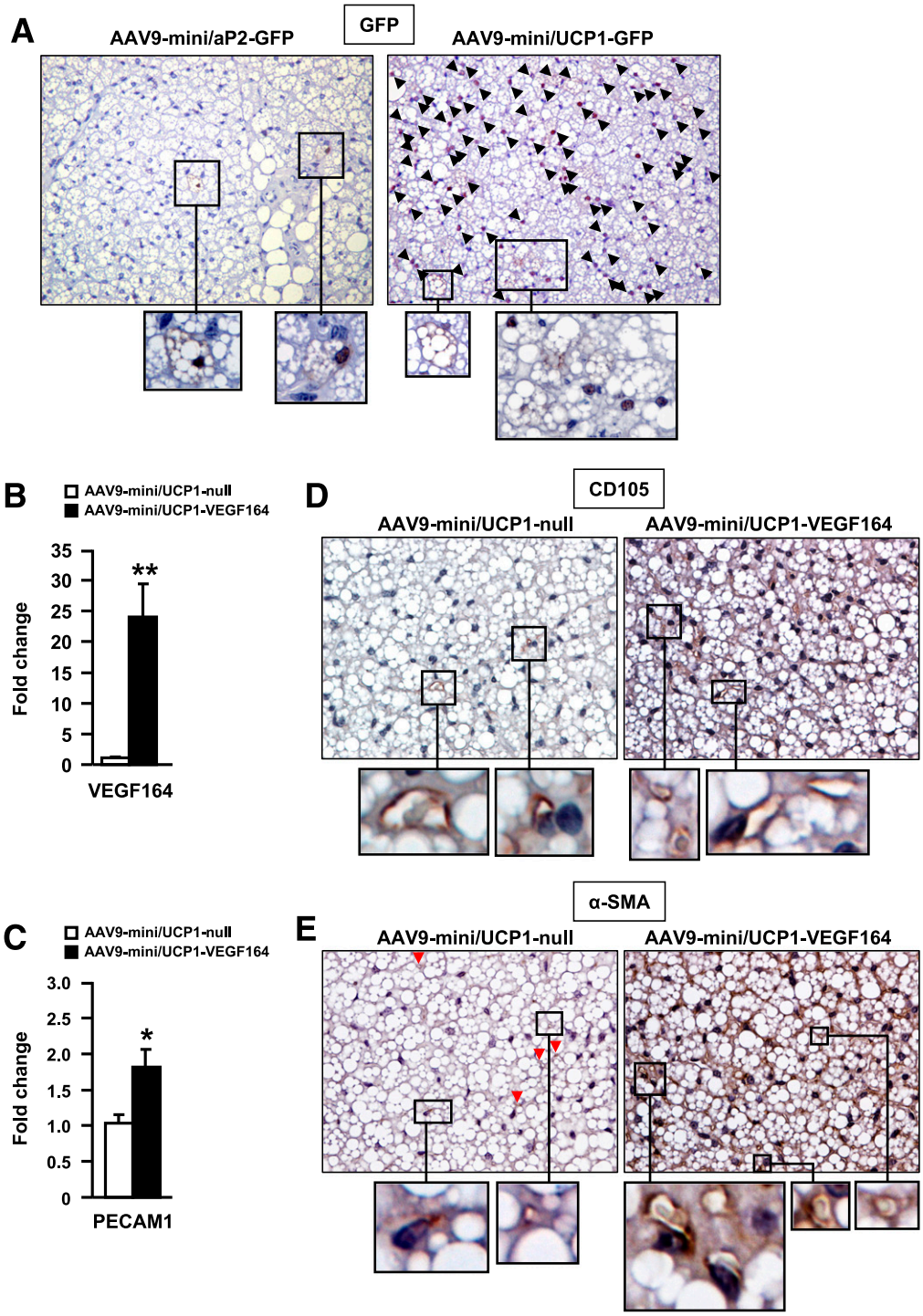

FIG. 6. Specific transduction of adipocytes after systemic administration of AAV vectors. *A*: Immunostaining against GFP (brown) in iBAT 2 weeks after systemic delivery of 2×10^{12} vg of AAV9-mini/aP2-GFP or AAV9-mini/UCP1-GFP vectors. The arrowheads indicate transduced brown adipocytes. Original magnification ×200 and ×400 (*insets*). VEGF164 (*B*) and PECAM1 (*C*) expression levels in iBAT 1 month after the intravascular administration of 8×10^{12} vg of AAV9-mini/UCP1-VEGF164 or AAV9-mini/UCP1-null vectors ($n = 5$). Immunostaining against CD105 (brown) (*D*) and α-SMA (brown) (*E*) in the same cohorts as in *B* and *C*. The red arrowheads indicate vessels. Original magnification ×400 and ×1,000 (*insets*). Values shown are means ± SEM. *$P < 0.05$; **$P < 0.01$.

modification of murine adipose tissue in vivo. AAV-mediated genetic engineering of WAT and BAT represents a technological advance that may prove useful for the study of physiopathology of metabolic diseases as well as for the development of new therapeutic approaches for obesity and type 2 diabetes.

ACKNOWLEDGMENTS

This work was supported by grants from Ministerio de Economía y Competitividad, Plan Nacional I+D+I (SAF 2011-24698) and Generalitat de Catalunya (2009 SGR-224 and ICREA Academia), Spain, and from European

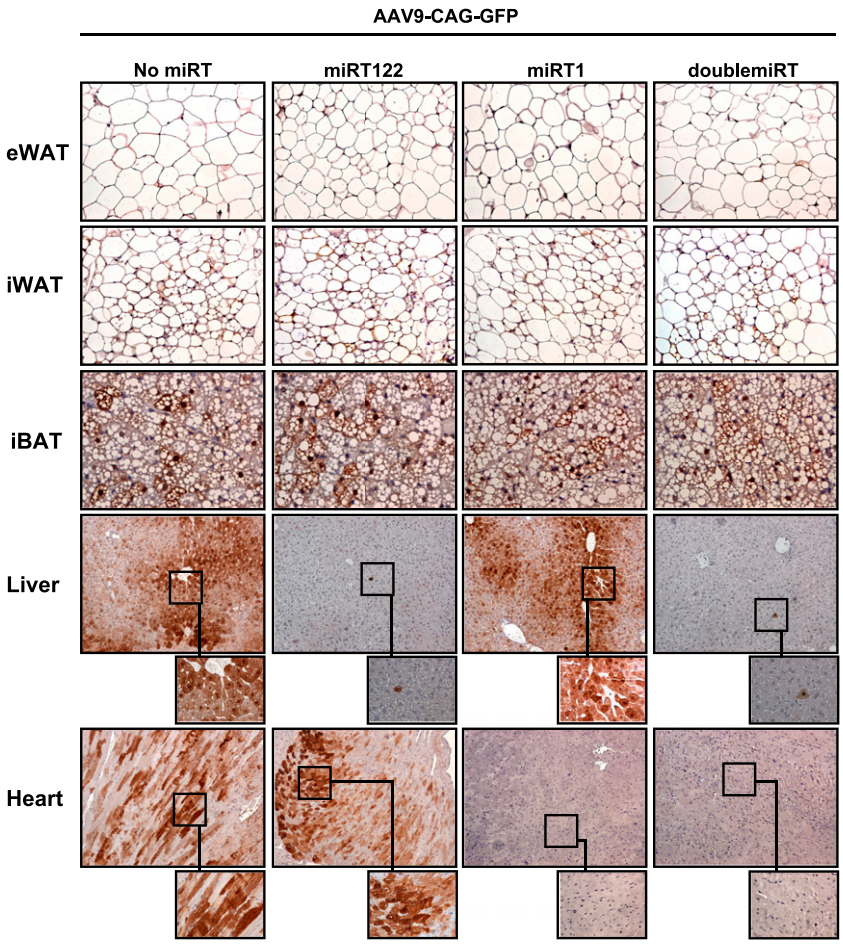

FIG. 7. Efficient adipocyte transduction and de-targeting of transgene expression from liver and heart with mirT sequences. GFP immunostaining (brown) in eWAT, iWAT, iBAT, liver, and heart at 2 weeks after intravascular administration of 10^{12} vg of AAV9-CAG-GFP, AAV9-CAG-GFP-miRT122, AAV9-CAG-GFP-miRT1, or AAV9-CAG-GFP-doublemiRT vectors. Original magnification ×100 (liver and heart), ×200 (eWAT and iWAT), and ×400 (iBAT and *insets*).

Commission DG Research FP6 (CLINIGENE, LSHB-CT-2006-018933). C.M. and E.C. were recipients of a predoctoral fellowship from the Ministerio de Educación, Cultura y Deporte, Spain.

No potential conflicts of interest relevant to this article were reported.

V.J. designed experiments, wrote and edited the manuscript, generated reagents, and performed experiments. S.M., E.C., C.M., I.E., C.J., A.R., and T.F. generated reagents and performed experiments. S.F. wrote and edited the manuscript, generated reagents, and performed experiments. F.B. designed experiments and wrote and edited the manuscript. F.B. is the guarantor of this work and, as such, had full access to all the data in the study and takes responsibility for the integrity of the data and the accuracy of the data analysis.

The authors thank Virginia Haurigot (Universitat Autònoma de Barcelona, Spain), Federico Mingozzi (Genethon, Evry, France), Malcolm Watford (Rutgers University, New Brunswick, NJ), and Miquel Garcia (Universitat Autònoma de Barcelona, Spain) for helpful discussions, and Marta Moya (Universitat Autònoma de Barcelona, Spain), Xavier Leon (Universitat Autònoma de Barcelona, Spain), Maria Molas (Universitat Autònoma de Barcelona, Spain), and Manuela Costa (SCAC, Universitat Autònoma de Barcelona, Spain) for technical assistance.

REFERENCES

1. Speakman JR, O'Rahilly S. Fat: an evolving issue. Dis Model Mech 2012;5:569–573
2. Moller DE, Flier JS. Insulin resistance—mechanisms, syndromes, and implications. N Engl J Med 1991;325:938–948
3. Spiegelman BM, Choy L, Hotamisligil GS, Graves RA, Tontonoz P. Regulation of adipocyte gene expression in differentiation and syndromes of obesity/diabetes. J Biol Chem 1993;268:6823–6826
4. Yen M, Ewald MB. Toxicity of weight loss agents. J Med Toxicol 2012;8:145–152
5. Cypess AM, Lehman S, Williams G, et al. Identification and importance of brown adipose tissue in adult humans. N Engl J Med 2009;360:1509–1517
6. Heilbronn LK, Campbell LV. Adipose tissue macrophages, low grade inflammation and insulin resistance in human obesity. Curr Pharm Des 2008;14:1225–1230
7. van Marken Lichtenbelt WD, Vanhommerig JW, Smulders NM, et al. Cold-activated brown adipose tissue in healthy men. N Engl J Med 2009;360:1500–1508
8. Meunier-Durmort C, Ferry N, Hainque B, Delattre J, Forest C. Efficient transfer of regulated genes in adipocytes and hepatoma cells by the combination of liposomes and replication-deficient adenovirus. Eur J Biochem 1996;237:660–667
9. Orlicky DJ, Schaack J. Adenovirus transduction of 3T3-L1 cells. J Lipid Res 2001;42:460–466
10. Quon MJ, Zarnowski MJ, Guerre-Millo M, de la Luz Sierra M, Taylor SI, Cushman SW. Transfection of DNA into isolated rat adipose cells by electroporation: evaluation of promoter activity in transfected adipose cells which are highly responsive to insulin after one day in culture. Biochem Biophys Res Commun 1993;194:338–346
11. Hertzel AV, Sanders MA, Bernlohr DA. Adenovirus-mediated gene transfer in primary murine adipocytes. J Lipid Res 2000;41:1082–1086

12. Forest C, Doglio A, Ricquier D, Ailhaud G. A preadipocyte clonal line from mouse brown adipose tissue. Short- and long-term responses to insulin and beta-adrenergics. Exp Cell Res 1987;168:218–232
13. Klaus S, Choy L, Champigny O, et al. Characterization of the novel brown adipocyte cell line HIB 1B. Adrenergic pathways involved in regulation of uncoupling protein gene expression. J Cell Sci 1994;107:313–319
14. Klein J, Fasshauer M, Klein HH, Benito M, Kahn CR. Novel adipocyte lines from brown fat: a model system for the study of differentiation, energy metabolism, and insulin action. Bioessays 2002;24:382–388
15. Soukas A, Socci ND, Saatkamp BD, Novelli S, Friedman JM. Distinct transcriptional profiles of adipogenesis in vivo and in vitro. J Biol Chem 2001;276:34167–34174
16. Blüher M. Transgenic animal models for the study of adipose tissue biology. Best Pract Res Clin Endocrinol Metab 2005;19:605–623
17. Fujimoto N, Matsuo N, Sumiyoshi H, et al. Adiponectin is expressed in the brown adipose tissue and surrounding immature tissues in mouse embryos. Biochim Biophys Acta 2005;1731:1–12
18. Urs S, Harrington A, Liaw L, Small D. Selective expression of an aP2/Fatty Acid Binding Protein 4-Cre transgene in non-adipogenic tissues during embryonic development. Transgenic Res 2006;15:647–653
19. Villarroya F, Brun S, Giralt M, Cámara Y, Solanes G, Iglesias R. Gene expression of leptin and uncoupling proteins: molecular end-points of fetal development. Biochem Soc Trans 2001;29:76–80
20. Endo T, Kobayashi T. Thyroid-stimulating hormone receptor in brown adipose tissue is involved in the regulation of thermogenesis. Am J Physiol Endocrinol Metab 2008;295:E514–E518
21. Granneman JG, Li P, Lu Y, Tilak J. Seeing the trees in the forest: selective electroporation of adipocytes within adipose tissue. Am J Physiol Endocrinol Metab 2004;287:E574–E582
22. Magovern CJ, Mack CA, Zhang J, Rosengart TK, Isom OW, Crystal RG. Regional angiogenesis induced in nonischemic tissue by an adenoviral vector expressing vascular endothelial growth factor. Hum Gene Ther 1997;8:215–227
23. Fradette J, Wolfe D, Goins WF, Huang S, Flanigan RM, Glorioso JC. HSV vector-mediated transduction and GDNF secretion from adipose cells. Gene Ther 2005;12:48–58
24. Mingozzi F, High KA. Therapeutic in vivo gene transfer for genetic disease using AAV: progress and challenges. Nat Rev Genet 2011;12:341–355
25. Mizukami H, Mimuro J, Ogura T, et al. Adipose tissue as a novel target for in vivo gene transfer by adeno-associated viral vectors. Hum Gene Ther 2006;17:921–928
26. Zhang FL, Jia SQ, Zheng SP, Ding W. Celastrol enhances AAV1-mediated gene expression in mice adipose tissues. Gene Ther 2011;18:128–134
27. Ayuso E, Mingozzi F, Montane J, et al. High AAV vector purity results in serotype- and tissue-independent enhancement of transduction efficiency. Gene Ther 2010;17:503–510
28. Graves RA, Tontonoz P, Spiegelman BM. Analysis of a tissue-specific enhancer: ARF6 regulates adipogenic gene expression. Mol Cell Biol 1992;12:1202–1208
29. Ross SR, Graves RA, Greenstein A, et al. A fat-specific enhancer is the primary determinant of gene expression for adipocyte P2 in vivo. Proc Natl Acad Sci U S A 1990;87:9590–9594
30. Cassard-Doulcier AM, Gelly C, Bouillaud F, Ricquier D. A 211-bp enhancer of the rat uncoupling protein-1 (UCP-1) gene controls specific and regulated expression in brown adipose tissue. Biochem J 1998;333:243–246
31. Larose M, Cassard-Doulcier AM, Fleury C, et al. Essential cis-acting elements in rat uncoupling protein gene are in an enhancer containing a complex retinoic acid response domain. J Biol Chem 1996;271:31533–31542
32. Muñoz S, Franckhauser S, Elias I, et al. Chronically increased glucose uptake by adipose tissue leads to lactate production and improved insulin sensitivity rather than obesity in the mouse. Diabetologia 2010;53:2417–2430
33. Pfaffl MW. A new mathematical model for relative quantification in real-time RT-PCR. Nucleic Acids Res 2001;29:e45
34. Franckhauser S, Muñoz S, Pujol A, et al. Increased fatty acid re-esterification by PEPCK overexpression in adipose tissue leads to obesity without insulin resistance. Diabetes 2002;51:624–630
35. Anguela XM, Tafuro S, Roca C, et al. Nonviral-mediated hepatic expression of IGF-I increases Treg levels and suppresses autoimmune diabetes in mice. Diabetes 2013;62:551–560
36. Elias I, Franckhauser S, Ferré T, et al. Adipose tissue overexpression of vascular endothelial growth factor protects against diet-induced obesity and insulin resistance. Diabetes 2012;61:1801–1813
37. Sung HK, Doh KO, Son JE, et al. Adipose vascular endothelial growth factor regulates metabolic homeostasis through angiogenesis. Cell Metab 2013;17:61–72
38. Fonsatti E, Nicolay HJ, Altomonte M, Covre A, Maio M. Targeting cancer vasculature via endoglin/CD105: a novel antibody-based diagnostic and therapeutic strategy in solid tumours. Cardiovasc Res 2010;86:12–19
39. Bergers G, Song S. The role of pericytes in blood-vessel formation and maintenance. Neuro Oncol 2005;7:452–464
40. Ruzo A, Marcó S, García M, et al. Correction of pathological accumulation of glycosaminoglycans in central nervous system and peripheral tissues of MPSIIIA mice through systemic AAV9 gene transfer. Hum Gene Ther 2012;23:1237–1246
41. Zincarelli C, Soltys S, Rengo G, Rabinowitz JE. Analysis of AAV serotypes 1-9 mediated gene expression and tropism in mice after systemic injection. Mol Ther 2008;16:1073–1080
42. Qiao C, Yuan Z, Li J, et al. Liver-specific microRNA-122 target sequences incorporated in AAV vectors efficiently inhibits transgene expression in the liver. Gene Ther 2011;18:403–410
43. Shingara J, Keiger K, Shelton J, et al. An optimized isolation and labeling platform for accurate microRNA expression profiling. RNA 2005;11:1461–1470
44. Lafontan M, Girard J. Impact of visceral adipose tissue on liver metabolism. Part I: heterogeneity of adipose tissue and functional properties of visceral adipose tissue. Diabetes Metab 2008;34:317–327
45. Sackmann-Sala L, Berryman DE, Munn RD, Lubbers ER, Kopchick JJ. Heterogeneity among white adipose tissue depots in male C57BL/6J mice. Obesity (Silver Spring) 2012;20:101–111
46. DiGirolamo M, Fine JB, Tagra K, Rossmanith R. Qualitative regional differences in adipose tissue growth and cellularity in male Wistar rats fed ad libitum. Am J Physiol 1998;274:R1460–R1467
47. Peinado JR, Jimenez-Gomez Y, Pulido MR, et al. The stromal-vascular fraction of adipose tissue contributes to major differences between subcutaneous and visceral fat depots. Proteomics 2010;10:3356–3366
48. Lee KY, Russell SJ, Ussar S, et al. Lessons on conditional gene targeting in mouse adipose tissue. Diabetes 2013;62:864–874
49. Haurigot,V, Marcó S, Ribera A, et al. Whole body correction of mucopolysaccharidosis IIIA by intracerebrospinal fluid gene therapy. J Clin Invest 2013;123:3254–3271
50. Callejas D, Mann CJ, Ayuso E, et al. Treatment of diabetes and long-term survival following insulin and glucokinase gene therapy. Diabetes 2013;62:1718–1729
51. McCaffrey AP, Fawcett P, Nakai H, et al. The host response to adenovirus, helper-dependent adenovirus, and adeno-associated virus in mouse liver. Mol Ther 2008;16:931–941
52. Stilwell JL, Samulski RJ. Role of viral vectors and virion shells in cellular gene expression. Mol Ther 2004;9:337–346
53. Martino AT, Suzuki M, Markusic DM, et al. The genome of self-complementary adeno-associated viral vectors increases Toll-like receptor 9-dependent innate immune responses in the liver. Blood 2011;117:6459–6468